Journal of System Design and Dynamics

Vol. 4, No. 6, 2010

Chaos-Entropy Analysis and Acquisition of Individuality and Proficiency of a Human Operator's Skill Using a Fuzzy Controller*

Yoshihiko KAWAZOE**, Keisuke ISHIKAWA*** and Yoshiaki IKURA***

**Department of Human-Robotics, Saitama Institute of Technology,
Fusaiji 1690, Fukaya, Saitama 369-0293, Japan
E-mail: kawazoe@sit.ac.jp

***Graduate School of Engineering, Saitama Institute of Technology

Abstract

In the present paper, we use time series data and fuzzy inference to identify individual differences in the behavior and proficiency of human operators performing various skills and use the identified individual skills as a fuzzy controller. Human operators are trained to a certain skill level at stabilizing an inverted pendulum, and the data obtained in 10 trials per operator were successively used for analysis, where the waveforms of pendulum angle and cart displacement were analyzed. The maximum Lyapunov exponents were estimated from time series data with respect to embedding dimensions. The fuzzy controller identified from the time series data for each trial and for each operator represented well the human-generated decision-making characteristics, exhibiting chaos and a large amount of disorder The estimated degree of freedom of motion increases and the estimated amount of disorder decreases with the increase in proficiency, both in the experiment and in the fuzzy control simulation. It is also revealed that the agreement between the experiment and the fuzzy control simulation for the degree of freedom of motion and indicates that the entropy ratio is particularly good when the measured waveform and the simulated waveform are similar in appearance.

Key words: Human Dynamics, Human Dexterity, Skill, Proficiency, Degree of Freedom of Motion, Amount of Disorder, Fuzzy Control, Chaos, Entropy, Identification, Time Series Data, Inverted Pendulum on a Cart

1. Introduction

Motion is a phenomenon that clearly indicates the living nature of a creature. Motion can be observed as a change in physical status. However, it is difficult to clarify how motion is acquired. There is an infinite variety of motions ranging from those of typical daily activities to the exceptional movement of an athlete or a musician[(1)].

Based on his extensive observation of child growth, Gesell (1945) stated some empirical rules. In particular, he noted that the development of motion progresses from a generally integrated state to an individualized state in which individual sections have specialized functions. He also noted that the number of degrees of freedom of motion increase with development and that periods of instability and stability continue to occur in order to advance the development by taking full advantage of such fluctuations. Finally, he observed that chaos plays a very important role in motion [(1)].

The human process of learning motion can also be studied by focusing on the degrees of freedom. When a person who normally writes with his or her right hand (i.e., their dominant hand) is asked to write with his or her left hand (i.e., their nondominant hand), the number of degrees of freedom of each joint is initially fixed. However, after training, each

*Received 30 Aug., 2010 (No. T2-09-0848)
Japanese Original : Trans. Jpn. Soc. Mech. Eng., Vol.76, No.765, C (2010), pp.1362-1371 (Received 24 Sep., 2009)
[DOI: 10.1299/jsdd.4.953]

joint moves according to a peculiar phase relationship after training (Newell & Van Emmerik, 1989). This implies that we are inflexible when attempting a new motion but become more relaxed after becoming accustomed to the new motion. The term "relax" in sports refers to a freeing of the degrees of freedom (DOF). In order to achieve a new motion, it is considered necessary to initially stiffen the body or to freeze the number of degrees of freedom [(1) - (3)].

Figure 1 shows a series of photographs taken by the authors showing "the movement of a cake craftsman" presented by Yoshinori Kono, where Fig. 1(a) shows the movement with a large number of degrees of freedom and Fig. 1(b) shows the movement with a small number of degrees of freedom.

Figure 2 shows a series of photographs taken by the authors showing the chaos and disorder in an electro-magnetically excited double pendulum (a toy), where Fig. 2(a) shows an example of a rotational period of 0.51 s and Fig. 2(b) shows an example of a rotational period of 0.70 s under the same condition. This means a complex system accompanied by regularity and disorder. If we define the essence of robotics as the development from mechanical engineering to dynamics and the control of a nonlinear multi-link system with large fluctuations, in which chaos occurs even in a two-link system, then research on the nonlinear dynamics and control of a robot is undeveloped. Although recent related research has examined, for example, delayed feedback control, only simulations with two-DOF links have been reported [(4)].

Figure 3 shows the experimental setup. An inverted pendulum is mounted on a cart that can move along the line of a sliding rail of limited length. The pendulum is attached to the rail such that the pendulum rotates in one plane. A human operator manipulates the cart directly by hand. Although some time and intensive training in needed in order for a human operator to succeed in stabilizing the pendulum for 60 s, this task becomes less difficult after the first successful instance of stabilization. The human operators in the experiment

(a) with a large number of degrees of freedom

(b) with a small number of degrees of freedom

Fig. 1 "Movement of a cake craftsman" presented by Yoshinori Kono.

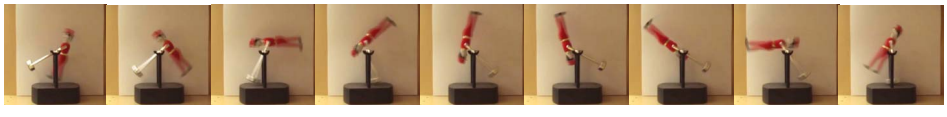

(a) Rotational period: 0.51 s

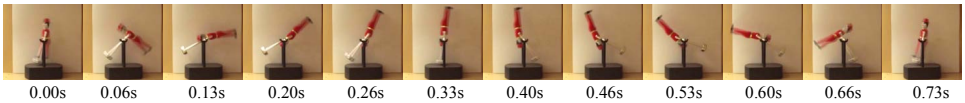

(b) Rotational period: 0.70 s

Fig. 2 Chaos and disorder in the excited double pendulum.

were trained so that they were skilled to a certain extent in stabilizing the pendulum, and the data obtained in 10 successive trials per person were used for analysis. The angle that the pendulum makes with the vertical axis and the displacement of the cart were measured, and the derivatives and the force that moves the cart can be derived based on these quantities [2][3].

In previous papers [2] [3] [5] [6], various nonlinear features were found in the stabilizing behavior of a human operator. In the present study, the definition of nonlinear stability indicates that an inverted pendulum does not fall for 60 consecutive seconds. The behavior during stabilizing control of an inverted pendulum by a human operator exhibits a random-like or limit-cycle-like fluctuation, and stabilizing control by a human operator is robust against disturbances. This may be because the limit-cycle-like fluctuation, which indicates linear instability, is more robust against disturbances than the linearly stable fluctuation produced by the digital PID computer controller (Fig. 4). The limit cycle was very stable with respect to nonlinearity, which means that the limit cycle is robust against disturbances. These observations suggest that active control is not necessary for small fluctuations of the inverted pendulum angle from the vertical position and is only necessary when the inverted pendulum angle exceeds a certain threshold. Here, motion control is discontinuous and intermittent, and the thresholds are very complex. Figure 5 shows

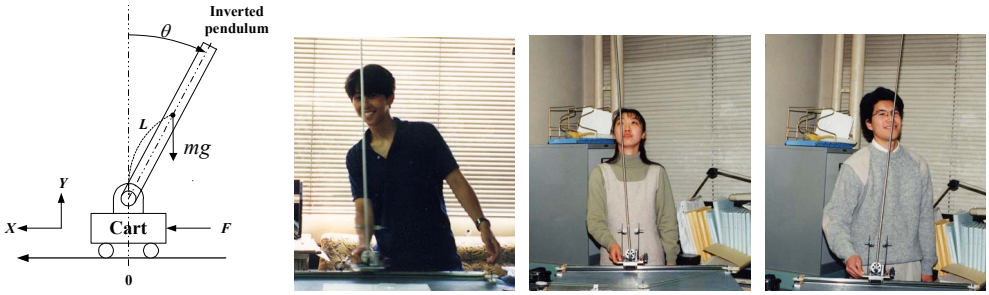

(a) (b)

Fig. 3 Stabilizing control of an inverted pendulum on a cart by a human operator.

Fig. 4 Stabilizing control of an inverted pendulum on a cart by a computer controller with PID

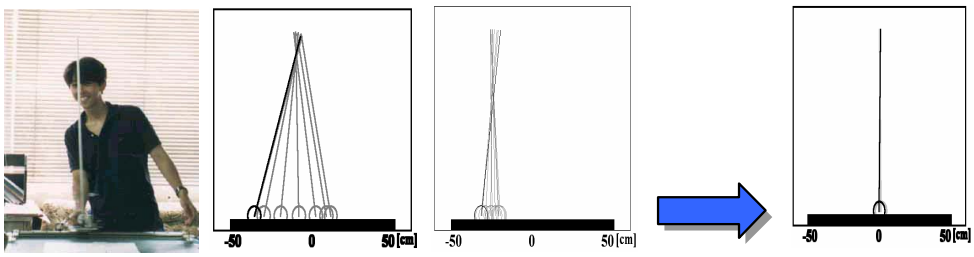

(a) unskilled (b) skilled

Fig.5 Skill building process of a human operator during stabilizing control of an inverted pendulum on a cart

schematically the skill building process of the human operator during stabilizing control of an inverted pendulum on a cart. The experiment revealed that the estimated number of degrees of freedom of a motion composed by a human operator and a control object increased and the estimated amount of disorder decreased as the number of trials increased. Furthermore, the neural network controller identified from the time series data for each trial and for each operator exhibited human-generated decision-making characteristics, which show chaos and a large amount of disorder. The neural control simulation confirmed that the estimated number of degrees of freedom of motion increases and the estimated amount of disorder decreases with the increase in the number of trials or the increase in proficiency. In addition, the agreement between the experimental results and the neural control simulation for the number of degrees of freedom and for the entropy ratios of motion were shown to be particularly good when the measured waveform and the simulated waveform are similar in appearance.

In the present paper, we use time series data and fuzzy inference to identify individual differences in the behavior and proficiency of human operators to acquire the individual skills of human operators. Furthermore, we investigate whether the fuzzy controller identified based on the time series data of each trial of each operator represents well the human-generated decision-making characteristics, exhibiting chaos and a large amount of disorder. In addition, we investigate both experimentally and through fuzzy control simulation whether the estimated number of degrees of freedom of motion will increase and the estimated amount of disorder will decrease with the increase in proficiency and whether the agreement between the experimental and fuzzy control simulation results for the number of degrees of freedom of motion and the entropy ratio is particularly good when the measured waveform and the simulated waveform are similar in appearance.

2. Fuzzy Identification and Fuzzy Control Simulation of Stabilizing Control of an Inverted Pendulum on a Cart by a Human Operator

Fuzzy control has a distinguishing feature in that it can incorporate experts' control rules using linguistic expressions. One of the main problems of fuzzy control is the difficulty in acquiring fuzzy rules and tuning the membership functions. The conventional control theory used to design controllers using models of controlled objects has been established. In addition, a number of studies have examined the design of fuzzy control systems using fuzzy models of controlled objects [7].

To identify the nonlinear characteristics of the human operator from the experimental time series data, we choose the pendulum angle θ_t, angular velocity θ'_t, and the cart displacement X_t and its velocity X'_t as input variables and the force F_t that moves the cart as the output of the fuzzy controller. Furthermore, we choose the combined variables $\theta_t + \beta\theta'_t$ and $X_t + \gamma X'_t$ as inputs so as to reduce the complexity of the control rule table, where β and γ are combination variables.

The method used to obtain the membership functions and the control rules are described in the following. The values of β and γ are identified using the identification of membership functions and control rules by a trial and error method after repeating several simulations. In order to partition the data and determine the border of the data with the fuzzy sets for the assumed values of coefficient β and γ, for example, G_{NB} = 10%, G_{NS} = 25%, G_{ZR} = 30%, G_{PS} = 25%, and G_{PB} = 10% were chosen (Fig. 6), and the borders were denoted by $D_{NB\,NS}$, $D_{NS\,ZR}$, $D_{ZR\,PS}$, and $D_{PS\,PB}$.

The labels of the membership functions with $\theta + \beta\theta'$ and $X + \gamma X'$ were determined as follows:

NB = minimum of the data: D_{MIN}, *NS* = $(D_{NB\,NS} + D_{NS\,ZR})/2$, *ZR* = mean of the data: D_{AVE}, *PS* = $(D_{ZR\,PS} + D_{PS\,PB})/2$, *PB* = maximum of the data: D_{MAX} (Fig. 7).

The labels of the membership function with *F* are also determined as follows:

NB = minimum of the data: D_{MIN}, *NMB* = (*NB* + *NS*)/2, *NS* = ($D_{NB\,NS}$ + $D_{NS\,ZR}$)/2, *NMS* = *NS*/2, *ZR* = average of the data: D_{AVE}, *PMS* = *PS*/2, *PS* = ($D_{ZR\,PS}$ + $D_{PS\,PB}$)/2, *PMB* = (*PB* + *PS*)/2, *PB* = maximum of the data: D_{MAX} (Fig. 8).

Suppose that $\theta_t + \beta\theta'_t$ is G_{NB}, $X_t + \gamma X'_t$ is G_{ZR}, and F_{t+1} is G_{NS}. Then, we count to the cell of label *F* = *NS* in the numbered grid to which $\theta + \beta\theta'$ = *NB* and $X + \gamma X'$ = *ZR* are given as inputs. Figure 9 shows the fuzzy output grid numbers for generating a control rule. The output is derived using the label frequencies of each grid for each trial and for each human operator and using the following equation:

$$F_{\mathrm{OUT}} = \frac{(-4.4\cdot \mathrm{NB})+(-2.0\cdot \mathrm{NS})+(0.0\cdot \mathrm{ZR})+(2.0\cdot \mathrm{PS})+(4.4\cdot \mathrm{PB})}{\mathrm{NB}+\mathrm{NS}+\mathrm{ZR}+\mathrm{PS}+\mathrm{PB}}. \quad (1)$$

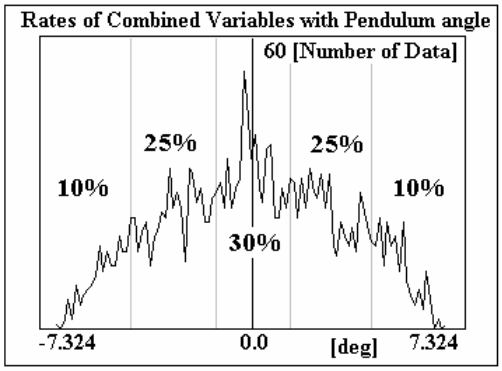

(a) Rates of combined variables with pendulum angle $\theta_t + \beta\theta'_t$

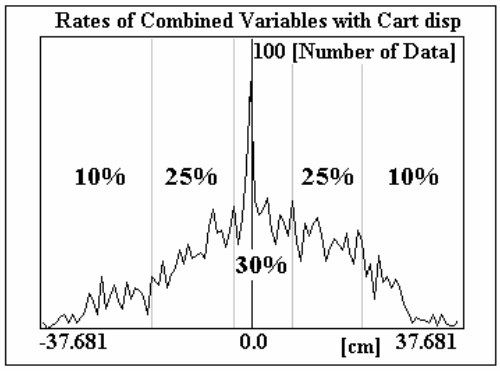

(b) Rates of combined variables with cart displacement $X_t + \gamma X'_t$

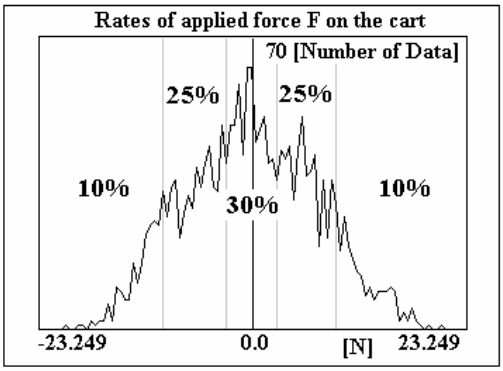

(c) Rates of applied force *F* on the cart

Fig.6 Example of rates of inputs and output. In order to partition the data and determine the border of the data with the fuzzy sets, G_{NB} = 10%, G_{NS} = 25%, G_{ZR} = 30%, G_{PS} = 25%, and G_{PB} = 10% were chosen.

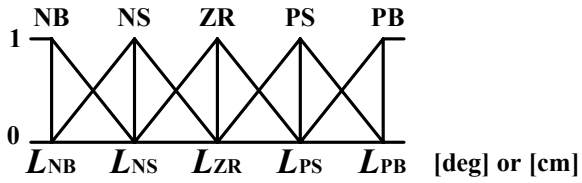

Fig. 7 Membership function for inputs.

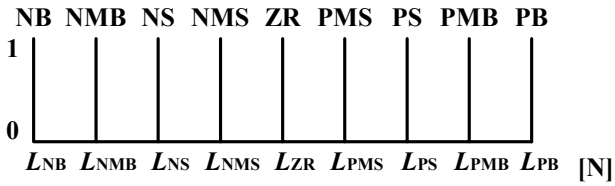

Fig. 8 Membership function (singleton) for output.

$X+\gamma X'$ \ $\theta+\beta\theta'$	N B	N S	Z R	P S	P B
N B	1	2	3	4	5
N S	6	7	8	9	10
Z R	11	12	13	14	15
P S	16	17	18	19	20
P B	21	22	23	24	25

Fig. 9 Fuzzy output grid number for generating a control rule.

Output Label	N B	NM B	NS	NM S	ZR	PMS	PS	PMB	PB
F_{OUT}	-3.5	-2.5	-1.5	-0.5	0.5	1.5	2.5	3.5	

Fig. 10 Conformity of output F_{out}.

$X+\gamma X'$ \ $\theta+\beta\theta'$	NB	NS	ZR	PS	PB
NB	PS	PMS	NMS	NMB	ZR
NS	PMB	PMS	NMS	NMB	ZR
ZR	PB	PS	ZR	NS	NB
PS	ZR	PMB	PMS	NMS	NMB
PB	ZR	ZR	PMS	NMS	NS

Fig. 11 Rule for control of a pendulum on a cart (first trial NK01 of human operator NK).

We can determine the output label using Fig. 10 and construct the operator's control rule for balancing the inverted pendulum as shown in Fig. 11.

Figure 12 shows a block diagram of the stabilizing control simulation of the pendulum on a cart using the constructed fuzzy controller from the time series data of the human operator.

Figure 13 shows the conformity of $\theta+\beta\theta'$, and Fig. 14 shows the conformity of $X+\gamma X'$, if $\theta + \beta\theta' = 4.0$ degrees and $X+\gamma X' = 5.0$ cm, as an example. In Fig. 13, the conformity of PS is determined to be 0.70, and that of PB is determined to be 0.30. In Fig. 14, the conformity of ZR is determined to be 0.73, and that of PS is determined to be 0.27. Using the fuzzy rule in Fig. 11, the following rules are found:

$$
\begin{aligned}
&IF \quad \theta + \beta\theta' = \mathbf{PS} \; and \; X + \gamma X' = \mathbf{ZR} \; \; THEN \quad F = \mathbf{NS} \\
&\qquad else \\
&IF \quad \theta + \beta\theta' = \mathbf{PS} \; and \; X + \gamma X' = \mathbf{PS} \; \; THEN \quad F = \mathbf{NMS} \\
&\qquad else \\
&IF \quad \theta + \beta\theta' = \mathbf{PB} \; and \; X + \gamma X' = \mathbf{ZR} \; \; THEN \quad F = \mathbf{NMB} \\
&\qquad else \\
&IF \quad \theta + \beta\theta' = \mathbf{PB} \; and \; X + \gamma X' = \mathbf{PS} \; \; THEN \quad F = \mathbf{NMB}
\end{aligned}
$$

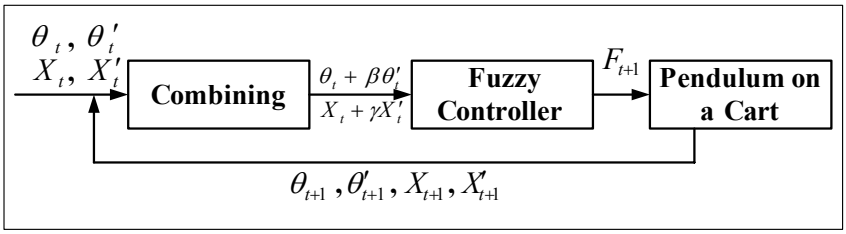

Fig.12 Stabilizing control simulation of the pendulum using the constructed fuzzy controller from the time series data of a human operator.

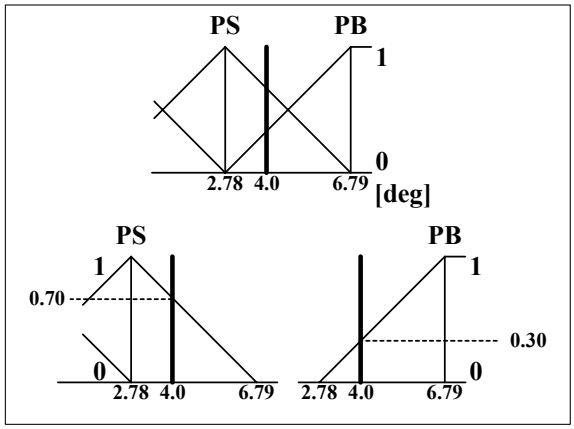

Fig. 13 Conformity of $\theta + \beta\theta'$.

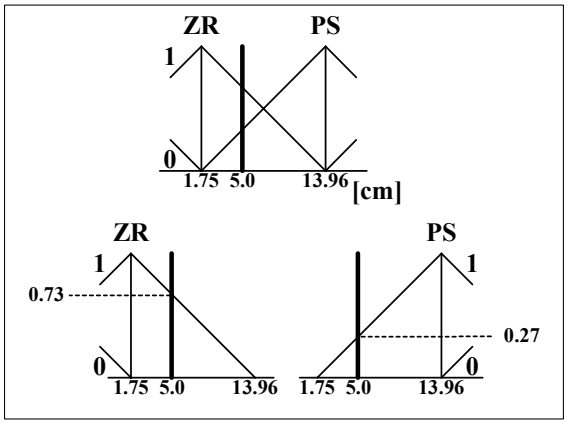

Fig. 14 Conformity of $X + \gamma X'$.

The output values are derived using max-min composition as follows. We use singleton fuzzification as a membership function of output. Figure 15 shows the process called "cutting" by MIN value. Figure 16 shows the process of composition by MAX value. Thus, the membership functions of output referred to as composite fuzzy output are obtained as NMB: 0.30, NS: 0.70, and NMS: 0.27. The output values are calculated using the center of

gravity method as follows:

$$F_{\mathrm{OUT}} = \frac{\sum_{i=1}^{9} X_i \cdot Y_i}{\sum_{i=1}^{9} Y_i}, \tag{2}$$

where the term X_i is the X coordinate (-20.46, -13.37, -6.27, -3.14, -0.02, 3.09, 6.18, 14.72, 23.25) of the output membership function, Y_i is the composite conformity, and i denotes an index. The result of fuzzy inference, F = -7.28, is obtained using composite fuzzy output in Fig. 16.

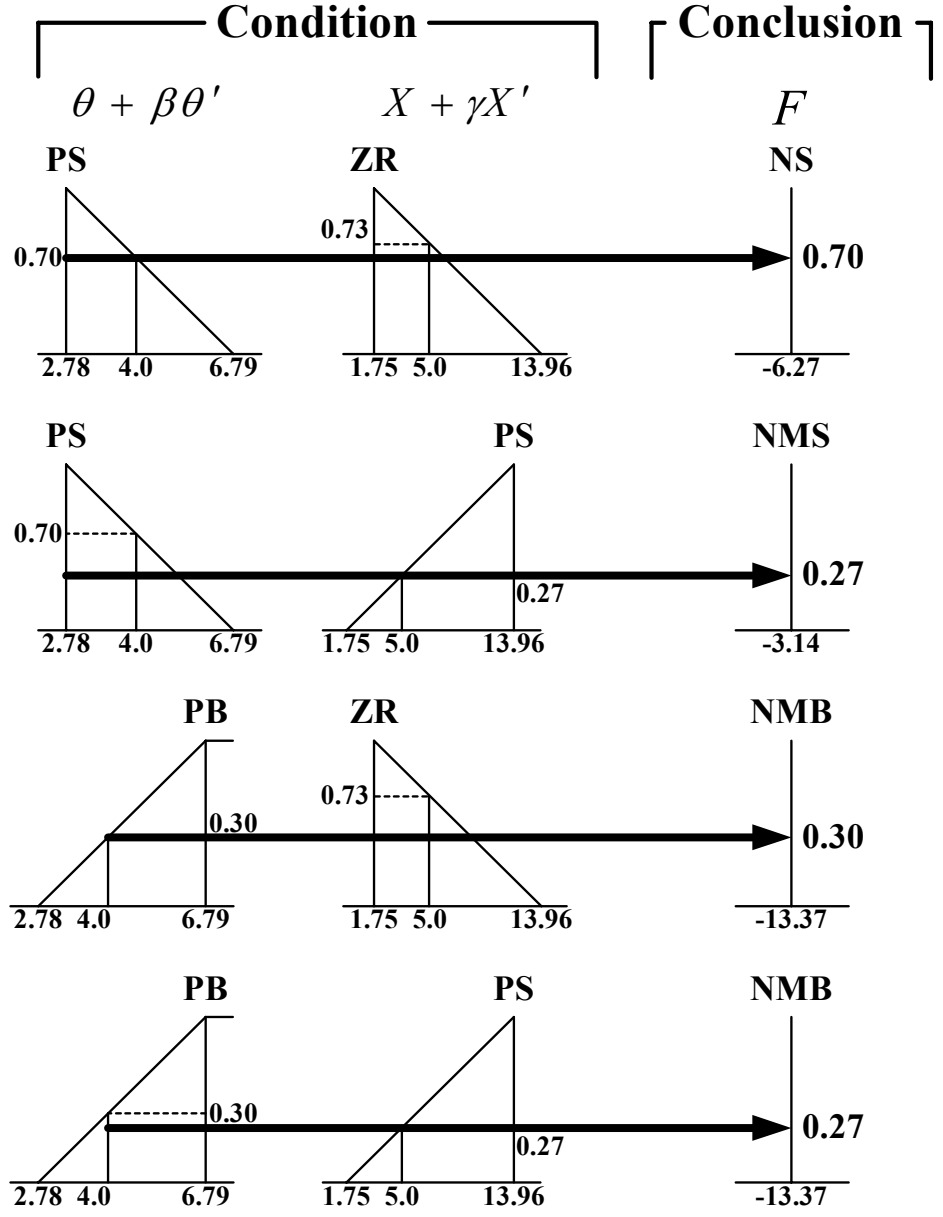

Fig.15 Cutting by MIN value.

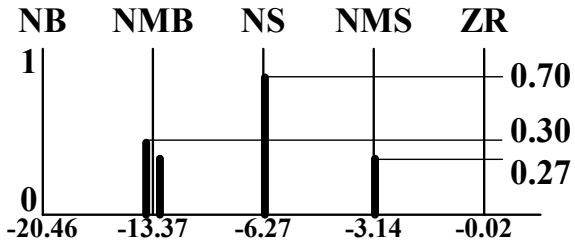

Fig.16 Composition by MAX value.

The differential equation of motion of this pendulum-cart system is described as follows:

$$M\ddot{X} - mL\ddot{\theta}\cos\theta + mL\dot{\theta}^2\sin\theta + \mu_x\dot{X} = F \quad (3)$$

$$I\ddot{\theta} - mL\ddot{X}\cos\theta + \mu_\theta\dot{\theta} = mgL\sin\theta \quad (4)$$

where m denotes the mass of the pendulum; M denotes the mass of the pendulum, the cart, and a human arm; L is the half-pendulum length; I is the inertial moment of pendulum about the supporting point; F is the force that moves the cart, μ_θ is the frictional coefficient of the pendulum support point, and μ_X is the frictional coefficient between the cart and the rail. The coefficients $\mu_\theta$and μ_X are derived from the experiment. The sampling time for control is 0.06 s, and the initial pendulum angle is 3.0 degrees.

3. Chaos-Entropy Analysis of a Human Operator's Skill during Stabilizing Control of an Inverted Pendulum on a Cart

In order to stabilize an unstable system, such as an inverted pendulum, strict judgment of the situation is required. Accordingly, it is expected that human operators exhibit complex behaviors or contingencies, i.e., a mixture of regular and random actions intermittently [(2)(3)(5)(6)].

Consider a hypothetical statistical system in which the outcome of a certain measurement must be located on a unit interval. If a line is subdivided into N subintervals, then we can associate a probability p_i with the i-th subinterval containing a particular range of possible outcomes. The entropy of the system is then defined as follows:

$$S = -\sum_{i=1}^{Nc} p_i \ln p_i \,. \quad (5)$$

This quantity may be interpreted as a measure of the amount of disorder in the system or as the information necessary to specify the state of the system. If the subintervals are equally probable, so that $p_i = 1/N$ for all i, then the entropy reduces to $S = \ln N$, which can be shown to be the maximum value. Conversely, if the outcome is known to be in a particular subinterval, then $S = 0$ is the minimum value. When $S = \log_e N$, the amount of further information needed to specify the result of a measurement is at a maximum, and, when $S = 0$, no further information is required [(8) - (10)]. We applied this formulation to the time series data by establishing N bins or subintervals of unit intervals into which the values of the time series data may fall. We define S as the net entropy calculated using Eq. (1) and $S/(\log_e N)$ as the entropy ratio [(11) - (13)]. The ratio of entropy to maximum entropy was estimated at the point at which the ratio saturated as the number of partitioned cells increased.

The detection of the chaotic dynamics and the quantitative characterization of the chaotic dynamics when the model of the entire system is unknown requires the analysis of time series data. Although methods for dynamic analysis of time series data are currently under development, the following two-step process is commonly used at present: (1) reconstruction of the strange attracter of an unknown dynamic system from the time series, and (2) determination of certain invariant quantities of the system from the reconstructed attracter. It is possible to obtain the

dynamics from a single time series without reference to other physical variables [8] - [10]. A rigorous mathematical basis of this concept has been presented by Takens [14] and Mane [15].

Since the attracter dimension is unknown for time series data and the required embedding dimension M is unknown, it is important that the reconstruction be embedded in a space of sufficiently large dimension to represent the dynamics completely. Thus, the dimension of the embedding space is increased by increments of one. The attractor is reconstructed, and its largest Lyapunov exponent is calculated. The process is continued until the largest Lyapunov exponent is saturated with respect to the embedding dimensions, and the dimension, i.e., the degrees of freedom of the system behavior, is estimated. The largest Lyapunov exponent can be obtained from time series data using an algorithm presented by Wolf *et al.* [16]. The Lyapunov exponent can be used to obtain a measure of the sensitivity under the initial conditions. This measure of sensitivity is characteristic of chaotic behavior. If the Lyapunov exponent is positive, nearby trajectories diverge, and so the evolution is sensitive to initial conditions and therefore chaotic.

Consider the time series data $x(t_1)$, $x(t_2)$, …. Successive points in the phase space formed from time-delay coordinates can be written in vector form $\boldsymbol{X_i}$ as follows:

$$\begin{aligned}
\mathbf{X}_1 &= (x(t_1), x(t_1+\tau), \cdots, x(t_1+(m-1)\tau)) \\
\mathbf{X}_2 &= (x(t_2), x(t_2+\tau), \cdots, x(t_2+(m-1)\tau)) \\
\mathbf{X}_3 &= (x(t_3), x(t_3+\tau), \cdots, x(t_3+(m-1)\tau)) \\
&\vdots \\
\mathbf{X}_i &= (x(t_i), x(t_i+\tau), \cdots, x(t_i+(m-1)\tau)) \\
&\vdots \\
\mathbf{X}_N &= (x(t_N), x(t_N+\tau), \cdots, x(t_N+(m-1)\tau))
\end{aligned} \tag{6}$$

where the symbol τ denotes the time delay, and the symbol m denotes the embedding dimension.

The choice of an appropriate delay τ is important to the success of the reconstruction. If τ is too short, then the coordinates are approximately the same and the reconstruction is useless. If τ is too large, then the coordinates are so far apart as to be uncorrelated. If the system has some rough periodicity, then a value comparable to but somewhat less than that period is typically chosen. Since there is no simple rule for choosing τ in all cases, τ is occasionally adjusted until the results appear to be satisfactory. Time τ is typically some multiple of the spacing between the time series points [8]. We chose 7 times the spacing between the time series points, i.e., 7 × 0.0293 s, as the value of τ because the calculated largest Lyapunov exponents were not too sensitive to τ and because the curves of the largest Lyapunov exponents versus embedding dimensions were smooth within a reasonable range τ, whereas the dominant period of the experimental time series data was 0.5 to 1.0 s.

Since the time series is presumed (by hypothesis) to be the result of a deterministic process, each x_{n+1} is the result of a mapping. In other words, we have

$$x_{n+1} = f(x_n). \tag{7}$$

The differentiation of the above equation (using j instead of n) is approximated as

$$\frac{df(x_j)}{dx_j} = \frac{dx_{j+1}}{dx_j} = \frac{x_{j+1} - x_j}{x_j - x_{j-1}} = f'(x_j). \tag{8}$$

Thus, the general expression of the Jacobian matrices and the orthogonal vectors $\boldsymbol{b}_{ij}\,(i = 1,2,\cdots,m)$ can be obtained [10]- [12] [16]. The Lyapunov exponents λ_i for each

embedding dimension i are then obtained as [8][10][14] - [16][19]

$$\lambda_i = \frac{1}{t_n - t_0} \sum_{j=1}^{n-1} \log_e \boldsymbol{b}_{ij} \quad (i = 1,2,3,\cdots,m). \tag{9}$$

where n denotes the number of data, t_0 the start of time and t_n the end of time.

The calculated largest Lyapunov exponent converges at the end of the time series data as the embedded dimensions increase. The number of degrees of freedom of motion are estimated by the dimensions when the curves of the largest Lyapunov exponents are saturated with respect to the embedding dimensions.

4. Chaos-Entropy Analysis and Acquisition of Individuality and Proficiency Using a Fuzzy Controller

Entropy can be interpreted as a measure of the amount of disorder in the system, and the maximum entropy can be interpreted as a random process with a uniform probability.

Figure 17 shows the entropy ratio vs. number of trial for human operators NK and Ot. According to the results for the estimated entropy ratio, the simulated time series data have a large amount of disorder. The estimated entropy ratio of motion increases with the increase in proficiency.

Figure 18 shows the estimated dimension (degrees of freedom) of motion vs. the number of trials for operators NK and OT. The estimated number of degrees of freedom of motion increases with the increase in proficiency.

Figures 19-1 and 19-2 show examples of simulated waveforms with the identified fuzzy

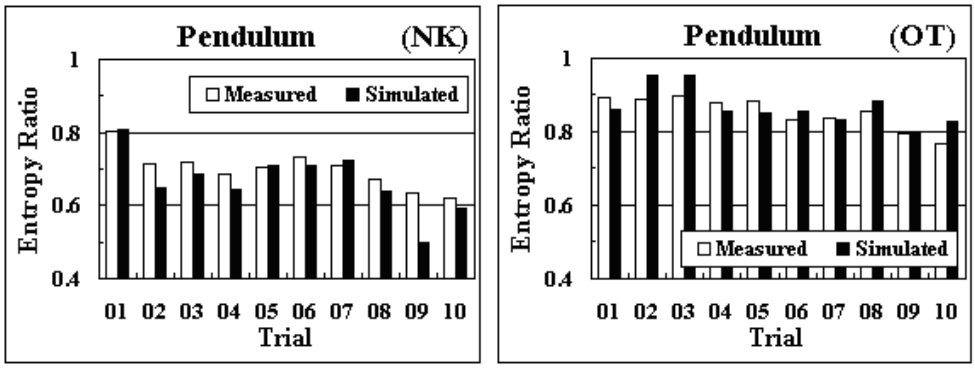

(a) Human operator NK (b) Human operator OT

Fig. 17 Entropy ratio vs. number of trials by human operators (measured and simulated with the identified fuzzy controller).

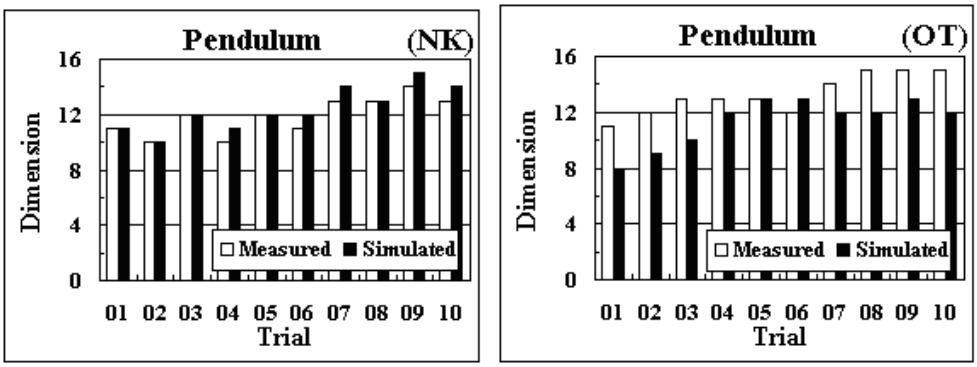

(a) Human operator NK (b) Human operator OT

Fig. 18 Estimated dimension (degrees of freedom) of motion vs. number of trials by human operators (measured and simulated with the identified fuzzy controller).

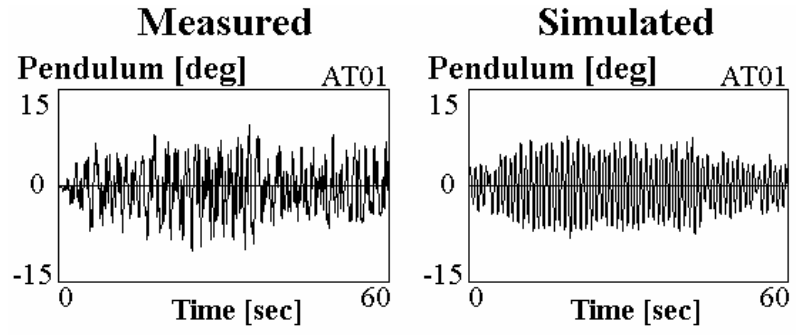

(a) Operator AT

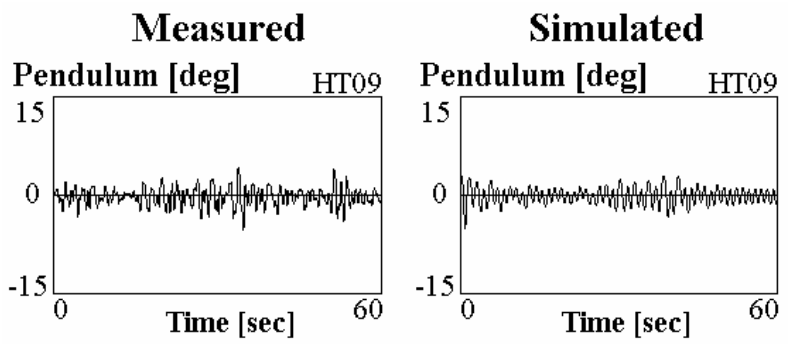

(b) Operator HT

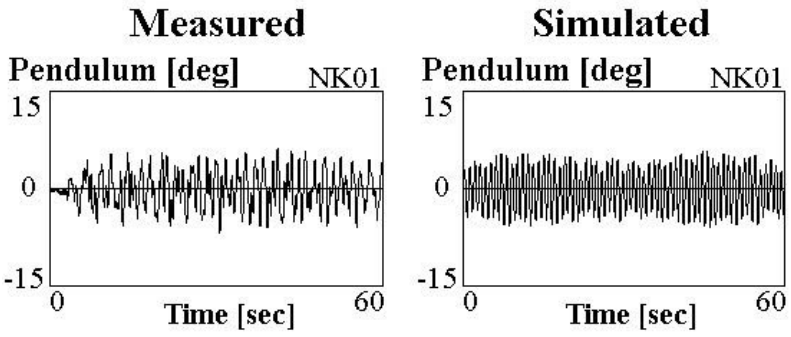

(c) Operator NK

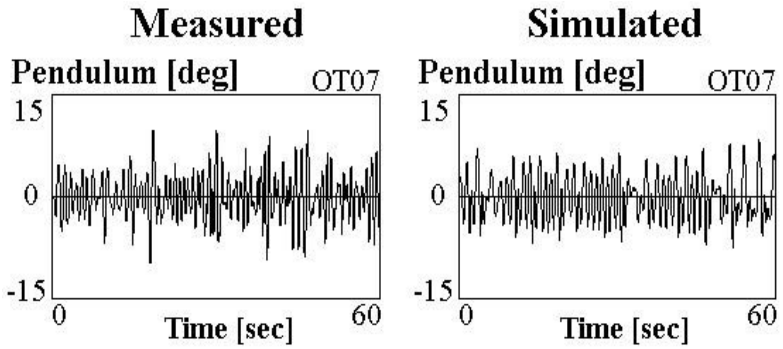

(d) Operator OT

Fig.19-1 Examples of simulated waveforms with the identified fuzzy controller and measured waveforms that are similar in appearance for eight human operators.

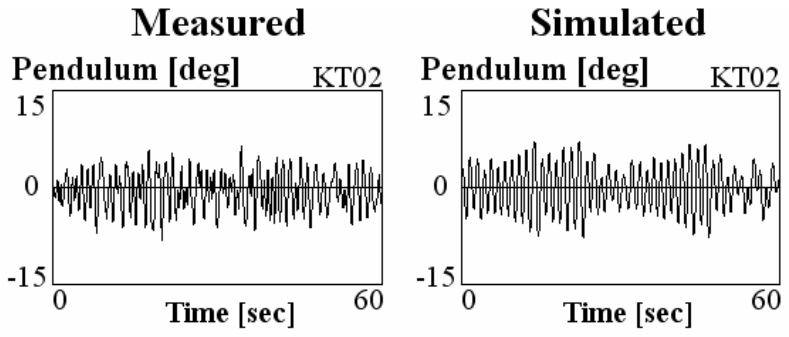

(e) Operator KT

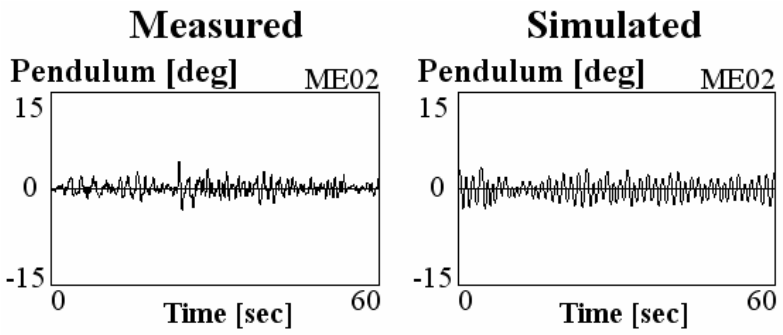

(f) Operator ME

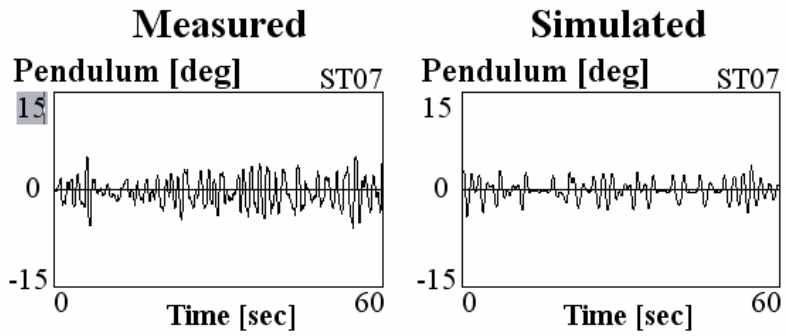

(g) Operator ST

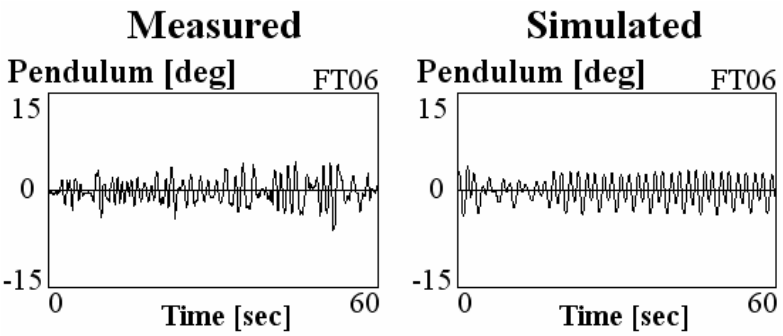

(h) Operator FT

Fig.19-2 Examples of waveforms simulated with the identified fuzzy controller and measured waveforms that are similar in appearance for eight human operators.

controller and measured waveforms that are similar in appearance for eight human operators.

Figure 20 shows the entropy ratios for eight human operators and for simulations using an identified fuzzy controller to produce similar waveforms.

Figure 21 shows the estimated dimension (degrees of freedom) for eight human operators and for simulations using an identified fuzzy controller to produce similar waveforms. The agreement between the simulated and experimental values for the number of degrees of freedom of motion and the entropy ratio is particularly good when the simulated waveform and the measured waveform are similar in appearance[2][3].

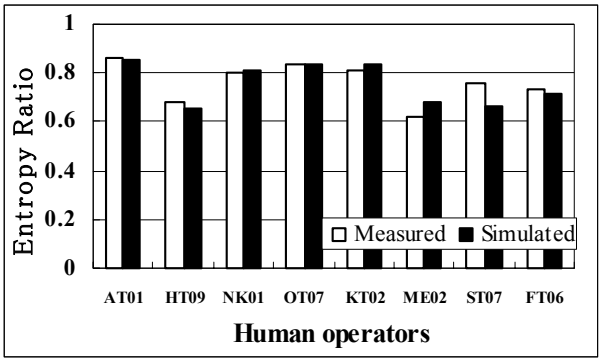

Fig.20 Entropy ratios for eight human operators and for simulations using an identified fuzzy controller to produce similar waveforms.

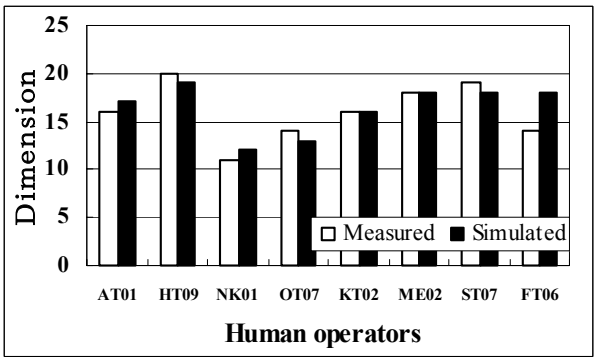

Fig.21 Estimated dimension (degree of freedom) for eight human operators and for simulations using an identified fuzzy controller to produce similar waveforms.

5. Conclusions

In the present paper, we have demonstrated that the fuzzy controller identified from the measured time series data for each trial for each human operator clearly exhibited the human-generated decision-making characteristics, exhibiting chaos and a large amount of disorder. We have also shown that the estimated number of degrees of freedom of motion increases and the estimated amount of disorder decreases with the increase in proficiency in the fuzzy control simulation. In addition, we have shown that the agreement between the experimental results and the fuzzy simulation for the number of degrees of freedom and for the entropy ratio of motion is particularly good when the measured waveform and the simulated waveform are similar in appearance. Accordingly, it was clarified that a simple fuzzy controller can be very useful for identifying the individuality and proficiency of a human operator when stabilizing an unstable system.

At present, despite notable differences in the behaviors of machinery and human beings, most research on man-machine systems has dealt with the linear characteristics of human behavior. There appear to be few studies and a number of unknowns regarding both the nonlinear characteristics of human behavior in an inherently unstable man-machine system

and the learning process of human operators for objects that are difficult to control [2][3].

The excessive number of degrees of freedom appears to provide considerable advantages. In several cases, a more flexible instrument, which is certainly much more challenging to work with, has undeniable advantages that provide better results. An experienced master will always prefer an instrument with a greater number of degrees of freedom over an instrument that is easier to use but constrains the worker. For example, a bicycle is harder to control than a tricycle, but anyone who has mastered a bicycle will probably never want to ride a tricycle again. The bicycle is preferred because in the hands of an experienced rider, it is more flexible and maneuverable and becomes more stable than the tricycle. Similarly, lightweight children's skates with their wide blades are less flexible and maneuverable than narrow-bladed speed skates. The practical problem of acquiring dexterity occurs in the early stages of skill development. This fascinating and extremely important area can move us closer to the deepest, concealed caches of knowledge about the human brain and its function [20]. Real intelligence in autonomous robots appears to be expressed by dexterity in humans or other living creatures as complex systems, and research and development are required to realize intellectual autonomous robots.

In a special issue of "Theories for Robot Control", the theory required for future robot research is considered [21][22]. Confusion and doubt arise among individuals who are involved in robotics research and development for a long time because numerous robot control theories have been proposed.

Dexterous dynamic actions required for humanoid biped robots, for example, are difficult to achieve through the current standard control strategy for humanoid robots based on the asymptotic convergence to the successive desired states with small fluctuations. Thus, a new and alternative approach is necessary [5][6][23]-[25]. In the future, we would like to apply the simple nonlinear optimal control of various movements to make full use of instability as a source of driving force.

Acknowledgements

The authors would like to thank Y. Kono[26] of a Japanese traditional martial artist (visiting professor at Kobe College) and K. Wakasugi at the Community College of Seibu Department Stores, Ltd. for performing the physical exercise for the physical exercise analysis. The authors would also like thank the late Prof. K. Tanaka of the Special School at Saitama Institute of Technology for his suggestions and encouragement. Sincere thanks are also due to the numerous students of Saitama Institute of Technology who helped to complete the present study.

References

(1) Taga, G., Dynamic Design of Brain and Body, (2002), Kaneko Shobo. (in Japanese)
(2) Kawazoe, Y., Ikura, Y., Uchiyama, K., and Kaise, T., Chaos-Entropy Analysis and Acquisition of Individuality and Proficiency of Human Operator's Skill Using a Neural Controller, *Journal of System Design and Dynamics*, Vol. 2, No. 6, (2008), pp. 1351-1363.
(3) Kawazoe, Y., Ikura, Y., Kaise, T., and Matsumoto, J., Chaos-Entropy Analysis and Acquisition of Human Operator's Skill Using a Fuzzy Controller: Identification of Individuality During Stabilizing Control of an Inverted Pendulum, *Journal of System Design and Dynamics*, Vol. 3, No. 6, (2009), pp. 932-943.
(4) Liu, D. and Yamaura, H., Realization of Giant Swing Motions of a 2-DOF Link Mechanism Using Delayed Feedback Control, *Transactions of the Japan Society of Mechanical Engineers*, Vol. 76, No. 767, C, (2010), pp. 1700- 1707. (in Japanese)
(5) Kawazoe, Y., Specifications of a Robot That Coexists with Nature, Life, and Humans:

Emergence of NANBA Walk and Run of Humanoid Biped Robot GENBE Based on the Distributed Control of the Physical Body in a Martial Art, *Journal of the Faculty of Engineering, Saitama Inst. Tech*, Vol. 15, (2005), pp. 11-23. (in Japanese)

(6) Kawazoe , Y., How Should Be the Robot That Coexists with Nature, Life and Human: Mechanism of Robustness of Humanoid Biped Robot GENBE Based on the Distributed Control of the Physical Body in a Martial Art, *Journal of the Faculty of Engineering, Saitama Inst. Tech*, Vol. 15, (2005), pp. 25-32. (in Japanese)

(7) Hasegawa, T., Furuhashi, T. and Uchikawa Y., *Journal of Japan Society for Fuzzy Theory and Systems*, 7-2, (1995), pp. 413-431.

(8) Baker, G. L. and Gollub, J. P., Chaotic dynamics: an introduction, Cambridge University Press, (1996), pp. 86-87.

(9) Baierlein, R., Atoms and Information Theory, (1971), W. H. Freeman and Co., San Francisco, Chapter 3.

(10) Shimojyo, T., Introduction to Chaos Dynamics, Kindaikagakusha, (1992), pp. 86-95, pp. 107-111. (in Japanese)

(11) Kawazoe, Y., Ohta, T., Tanaka, K., and Nagai, K, Nonlinear Behavior in Stabilizing Control of an Inverted Pendulum on a Cart by a Human Operator: Remarks on Chaotic Behaviors and a Complex System, *Proc. of the 5th Symposium on Motion and Vibration Control*, No. 97-31 (1997.11), pp. 395-398. (in Japanese)

(12) Kawazoe, Y., Hashimoto, K., and Ohta, T., Nonlinear Characteristics of an Operator Behavior During Stabilizing Control of an Inverted Pendulum on a Cart. (1st., Fuzzy Identification of Individual Difference and Skill-Up Process from Experimental Time Series Data and Fuzzy Control Simulation, *Proc. of the Dynamics and Design Conference*, No. 98-8(B), (1998), pp. 168-171. (in Japanese)

(13) Kawazoe, Y., Nonlinear Characteristics of an Operator Behavior During Stabilizing Control of an Inverted Pendulum on a Cart: Fuzzy Identification of Individual Difference and Skill Up Process from Experimental Time Series Data and Fuzzy Control Simulation, *Proc. of the Dynamics and Design Conference*, No. 99 -7 (A), (1999), pp. 251-254. (in Japanese)

(14) Takens, F., Detecting strange attracters in turbulence, in Rand, D. A. and Young, L. S. (eds.), Lecture Notes in Mathematics, Vol. 898, pp. 366-381, (1981), Springer-Verlag, Berlin.

(15) Mane, R. On the dimension of the compact invariant sets of certain nonlinear maps, in Rand, D. A. and Young L. S. (eds.), ibid, Vol. 898, (1981), Springer Verlag, Berlin, pp. 230-242.

(16) Wolf, A., Swift, J. B., Swinney H. L., and Vastano J. A., Determining Lyapunov Exponents From a Time Series, *Physica*, 16D, (1985). pp. 285-317.

(17) Aihara, K., ed., Chaos Seminar, Kaibundo, (1993), pp.51 - 53, p.150. (in Japanese)

(18) Nagashima, H. and Baba, Y., Introduction to Chaos, Baihukan, p.89. (in Japanese)

(19) Kodera, H., Linear Algebra, Kyoritu Shuppan, Tokyo, p. 94. (in Japanese)

(20) Bernstein, N. A., Dexterity and its Development, Latash, M. and Turvey, M. (eds.), LEA Publishers, New Jersey, (1996).

(21) Shimada, A. and Oaki, J., On special issue "Theories for Robot Control", *J. of the Robotics Society of Japan*, Vol. 27, No. 4, (2009), p. 369. (in Japanese)

(22) Kajita, S., From Inverted Pendulums to Biped Locomotion—ZMP and control theory, *J. of the Robotics Society of Japan*, Vol. 27, No. 4, (2009), pp. 392-395. (in Japanese)

(23) Kuniyoshi, Y., Ohmura, Y., Terada, K., and Nagakubo, A., Dynamic Roll-and-Rise Motion by an Adult-Size Humanoid Robot, *J. of the Robotics Society of Japan*, Vol. 23, No. 6, (2005), p. 706-717.(in Japanese)

(24) Nazir, N., Nakaura, S., and Sampei, M., Performance Limitation on ZMP Feedback Control of Humanoid Robot, J. of the Robotics Society of Japan, Vol. 22, No. 5, (2004),

pp. 656-665. (in Japanese)

(25) Maruyama, J., Matsubara, T., Hale, J., and Morimoto, J., Learning Stepping Motions for Fall Avoidance with Reinforcement Learning, *J. of the Robotics Society of Japan*, Vol. 27, No. 5, (2009), pp. 656-665. (in Japanese)

(26) George Nishiyama (Editing by Sophie Hardach), Japan athletes, caregivers turn to art of samurai, http://www.reuters.com/article/idUST266297020080305, Reuters (2008),Tokyo Tue Mar 4.